

Asymmetric wave propagation in planar chiral fibers

Dana Shemuly,¹ Zachary M. Ruff,² Alexander M. Stolyarov,¹ Grisha Spektor,³ Steven G. Johnson,¹ Yoel Fink,¹ Ofer Shapira^{1,*}

¹Research Laboratory of Electronics, Massachusetts Institute of Technology, 77 Massachusetts Avenue, Cambridge, Massachusetts 02329-0407, USA

²OmniGuide Communications, One Kendall Sq. building 100, 3rd floor, Cambridge, Massachusetts 02139, USA

³Department of Electrical Engineering, Technion- Israel Institute of Technology, Haifa 32000, Israel

*ofers@mit.edu

Abstract: We demonstrate the realization of a two-dimensional chiral optical waveguide with an infinite translational symmetry that exhibits asymmetric wave propagation. The low-symmetry geometry of the cross-section that lacks any rotational and mirror symmetries shows *in-principal* directional asymmetric polarization rotation. We use general symmetry arguments to provide qualitative analysis of the waveguide's eigenstates and numerically corroborate this using finite element simulation. We show that despite the only perturbative break of time-reversal symmetry via small modal losses, the structure supports a non-degenerate pair of co-rotating elliptical modes. We fabricated meters long fiber with a spiral structure and studied its optical properties.

© 2013 Optical Society of America

OCIS codes: (060.2310) Fiber optics; (060.5295) Photonic crystal fibers; (230.7370) Waveguides.

References and links

1. I. Tinoco and M. P. Freeman, "The optical activity of oriented copper helices, I. Experimental," *J. Phys. Chem.* **61**(9), 1196–1200 (1957).
2. M. Decker, M. W. Klein, M. Wegener, and S. Linden, "Circular dichroism of planar chiral magnetic metamaterials," *Opt. Lett.* **32**(7), 856–858 (2007).
3. E. Plum, V. A. Fedotov, A. S. Schwanecke, N. I. Zheludev, and Y. Chen, "Giant optical gyrotropy due to electromagnetic coupling," *Appl. Phys. Lett.* **90**(22), 223113 (2007).
4. M. Thiel, M. S. Rill, G. von Freymann, and M. Wegener, "Three-dimensional bi-chiral photonic crystals," *Adv. Mater. (Deerfield Beach Fla.)* **21**(46), 4680–4682 (2009).
5. S. Zhang, Y. S. Park, J. Li, X. Lu, W. Zhang, and X. Zhang, "Negative refractive index in chiral metamaterials," *Phys. Rev. Lett.* **102**(2), 023901 (2009).
6. J. B. Pendry, "Time reversal and negative refraction," *Science* **322**(5898), 71–73 (2008).
7. A. Drezet, C. Genet, J. Y. Laluet, and T. W. Ebbesen, "Optical chirality without optical activity: How surface plasmons give a twist to light," *Opt. Express* **16**(17), 12559–12570 (2008).
8. F. D. M. Haldane and S. Raghu, "Possible realization of directional optical waveguides in photonic crystals with broken time-reversal symmetry," *Phys. Rev. Lett.* **100**(1), 013904 (2008).
9. Z. Wang, Y. D. Chong, J. D. Joannopoulos, and M. Soljacic, "Observation of unidirectional backscattering-immune topological electromagnetic states," *Nature* **461**(7265), 772–775 (2009).
10. J. K. Gansel, M. Thiel, M. S. Rill, M. Decker, K. Bade, V. Saile, G. von Freymann, S. Linden, and M. Wegener, "Gold helix photonic metamaterial as broadband circular polarizer," *Science* **325**(5947), 1513–1515 (2009).
11. V. A. Fedotov, P. L. Mladyonov, S. L. Prosvirnin, A. V. Rogacheva, Y. Chen, and N. I. Zheludev, "Asymmetric propagation of electromagnetic waves through a planar chiral structure," *Phys. Rev. Lett.* **97**(16), 167401 (2006).
12. J. D. Joannopoulos, S. G. Johnson, J. N. Winn, and R. D. Meade, *Photonic Crystals: Molding the Flow of Light*, (2nd ed. Princeton University Press, Princeton, Oxford, 2008).
13. J. A. Kong, *Electromagnetic Wave Theory* (EMW Publishing, Cambridge, Massachusetts, 2000).
14. L. Hecht and L. D. Barron, "Rayleigh and Raman optical activity from chiral surfaces," *Chem. Phys. Lett.* **225**(4-6), 525–530 (1994).

15. L. R. Arnaut and L. E. Davis, "Dispersion characteristics of planar chiral structure," in *Proceedings of the International Conference on Electromagnetics in Advanced Applications*, Swanley, UK, 1995 (Nexus Media), 381–388.
16. R. Singh, E. Plum, C. Menzel, C. Rockstuhl, A. K. Azad, R. A. Cheville, F. Lederer, W. Zhang, and N. I. Zheludev, "Terahertz metamaterial with asymmetric transmission," *Phys. Rev. B* **80**(15), 153104 (2009).
17. V. A. Fedotov, A. S. Schwanecke, N. I. Zheludev, V. V. Khardikov, and S. L. Prosvirnin, "Asymmetric transmission of light and enantiomerically sensitive plasmon resonance in planar chiral nanostructures," *Nano Lett.* **7**(7), 1996–1999 (2007).
18. E. A. Marcatili and R. A. Schmeltzer, "Hollow metallic and dielectric waveguides for long distance optical transmission and lasers," *Bell Syst. Tech. J.* **43**, 1783–1809 (1964).
19. P. Yeh, A. Yariv, and E. Marom, "Theory of Bragg fiber," *J. Opt. Soc. Am.* **68**(9), 1196–1201 (1978).
20. S. G. Johnson, M. Ibanescu, M. A. Skorobogatiy, O. Weisberg, J. D. Joannopoulos, and Y. Fink, "Perturbation theory for Maxwell's equations with shifting material boundaries," *Phys. Rev. E Stat. Nonlin. Soft Matter Phys.* **65**(6), 066611 (2002).
21. M. Skorobogatiy, S. A. Jacobs, S. G. Johnson, and Y. Fink, "Geometric variations in high index-contrast waveguides, coupled mode theory in curvilinear coordinates," *Opt. Express* **10**(21), 1227–1243 (2002).
22. B. Temelkuran, S. D. Hart, G. Benoit, J. D. Joannopoulos, and Y. Fink, "Wavelength-scalable hollow optical fibres with large photonic bandgaps for CO₂ laser transmission," *Nature* **420**(6916), 650–653 (2002).
23. K. Kuriki, O. Shapira, S. Hart, G. Benoit, Y. Kuriki, J. F. Viens, M. Bayindir, J. D. Joannopoulos, and Y. Fink, "Hollow multilayer photonic bandgap fibers for NIR applications," *Opt. Express* **12**(8), 1510–1517 (2004).
24. D. Shemuly, A. M. Stolyarov, Z. M. Ruff, L. Wei, Y. Fink, and O. Shapira, "Preparation and transmission of low-loss azimuthally polarized pure single mode in multimode photonic band gap fibers," *Opt. Express* **20**(6), 6029–6035 (2012).
25. C. Menzel, C. Helgert, C. Rockstuhl, E. B. Kley, A. Tünnermann, T. Pertsch, and F. Lederer, "Asymmetric Transmission of Linearly Polarized Light at Optical Metamaterials," *Phys. Rev. Lett.* **104**(25), 253902 (2010).
26. M. Thiel, M. Decker, M. Deubel, M. Wegener, S. Linden, and G. von Freymann, "Polarization stop bands in chiral polymeric three-dimensional photonic crystals," *Adv. Mater. (Deerfield Beach Fla.)* **19**(2), 207–210 (2007).

Chiral symmetry, a symmetry in which an object cannot be mapped into its mirror image with the use of only rotation or translation, can be found in nature in structures that span many length-scales, from sugar molecules to galaxies. Artificial sub-wavelength chiral structures have been demonstrated in the last century, exhibiting fascinating electromagnetic phenomena [1–7], some of which do not occur in chiral materials found in nature. In this letter, we show that spiral waveguide structures, as shown in Fig. 1(a), possess chiral properties, such as pairs of co-rotating elliptically polarized modes, whose handedness depends on the propagation direction, and yet the source of this chirality is fundamentally distinct from previous chiral work with non-reciprocal [8, 9] or three-dimensional helical [10] structures. Our investigation was inspired by the fact that many recent experimental realizations of concentric-ring Bragg fibers (Fig. 1(b)) actually produced spiral structures as a byproduct of the fabrication technique, and yet the new features introduced by the spiral's symmetry-breaking were not analyzed. For example, the pairs of linearly polarized degenerate modes in Bragg fibers are split into non-degenerate elliptically polarized modes, resulting from the *combination* of the lack of in-plane mirror symmetry (planar chirality) and the breaking of time-reversal symmetry by losses. But, unlike previous work that obtained elliptical modes in lossy planar-chiral materials [11], our modes have simultaneously low propagation losses (<5 dB/m) and strong ellipticity (ratio of major to minor ellipse's axes is around 3.3). Also, despite the fact that the exponential mode confinement in Bragg fibers ostensibly depends on the rotational symmetry to eliminate waves from escaping by azimuthal propagation [12], we show that the spiral structure nevertheless only slightly increases the waveguide losses. The spiral fiber represents, then, a meters long, flexible, low loss, optical device with properties of a planar-chiral structure. We analyze spiral waveguides theoretically from a symmetry perspective, computationally using finite-element simulations, and experimentally with fabrication and measurements that demonstrate "directional" properties of the modes.

Chirality refers to a lack of inversion symmetry in a structure, so that it differs from its mirror image, and this lack of symmetry is a precondition to obtain various types of "directional" effects in optics. The most dramatic directional phenomena are one-way

waveguides, which only support modes called “chiral edge states” propagating in a single direction [9], but such waveguides require magneto-optic materials that break electromagnetic reciprocity. If we restrict the analysis to reciprocal materials (such as dielectrics, with or without loss), then the theorem of reciprocity applies to any linear time-invariant geometry [13], and forbids one-way modes or optical isolators. However, purely geometric effects can give rise to elliptically polarized non-degenerate modes, which distinguish a “handedness” of the structure. One way to achieve such modes is by a three-dimensional chiral structure such as a helix, which has *no* mirror-symmetry planes: such structures can give rise to strongly elliptical polarizations even in the absence of loss, in which case time-reversal symmetry implies that a right-handed mode remains right-handed when propagating in the opposite direction (the “sense of twist” [11, 14, 15] is non-directional). On the other hand, one can have a planar chiral structure, which has a constant (xy) cross-section with no mirror symmetry in the cross section. Because such structures have a $z \rightarrow -z$ mirror-symmetry, however, they *cannot* have non-degenerate elliptical modes unless time-reversal symmetry is broken: mirror-flipping a mode results in a mode propagating in the opposite direction with the opposite handedness (opposite sense of twist), whereas time-reversal would give the same handedness. Without using magneto-optic materials, the only way to break time-reversal symmetry is to introduce losses. Although lossy planar-chiral geometries have been demonstrated to support elliptical polarizations [11], the elliptical modes in this previous work always had significant losses. Counter intuitively, we show in this letter that a spiral waveguide can support very strong ellipticity that arises from very small modal losses.

Figure 1(a) depicts a cross-section of the spiral fiber. The structure, which has infinite translation symmetry, is made from non-chiral materials. The unique properties of the eigenstates supported by such a waveguide, and hence light propagation in it, could be elucidated using general symmetry arguments. We will compare the symmetries of the spiral fiber to those of related systems: the 1D photonic band gap fiber (Bragg fiber) (Fig. 1(b)), and the circular hollow metallic waveguide (Fig. 1(c)). All three systems have continuous translational symmetry along the waveguide axis z , and mirror symmetry with respect to the r - ϕ plane ($z \rightarrow -z$). Both the metallic waveguide and the Bragg fiber also possess continuous rotational symmetry, inversion symmetry, and mirror symmetry with respect to the r - z plane. The spiral fiber, on the other hand, does not possess the rotational symmetry, the inversion symmetry, nor the mirror symmetry with respect to the r - z plane. Moreover, while both the metallic waveguide and Bragg fiber are invariant under 180° rotation around the r axis, the spiral fiber is not, which enables the directionality in this fiber. Though the fiber is directional, exhibiting asymmetry with respect to coupling direction, it is still reciprocal. The directionality is a consequence of the break of symmetry that results in a break of modes degeneracy and material losses. The origin of directionality in reciprocal structures was previously pointed out for several different 2D planar chiral structures [7, 11, 16, 17].

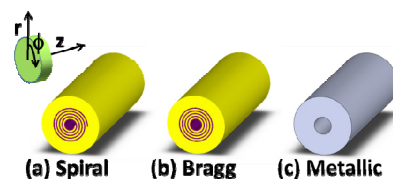


Fig. 1. A schematic description of the three cross-sections of the waveguides discussed: (a) The spiral fiber, (b) The hollow core 1D PBG fiber (Bragg fiber), and (c) The hollow core metallic waveguide. In all cases the core is hollow. The metallic waveguide, on the right, is made of hollow core and perfect metal walls. In the cases of the hollow Bragg fiber, center, and spiral fiber, left, the layers and the cladding with the light color (yellow) are low index of refraction material, and the layers with the dark color (purple) are the high index of refraction material. On the top left is a definition of the cylindrical coordinate system.

The modes of both the Bragg fiber and the metallic waveguide have been discussed extensively in the past (for example [18, 19]). In this paper we will highlight the main points that relate these modes to the symmetry of each structure and differentiate these modes from the modes of the spiral fiber. A summary is presented in Table 1. As in all cylindrical waveguides, all the modes in both the metallic waveguide and the Bragg fiber have three conserved quantities: the frequency ω , a result of the time translational symmetry and linearity of the system; the wave vector in the z direction k_z , a result of the continuous translational symmetry, T_∞ ; and the angular momentum m , a result of the continuous rotational symmetry, C_∞ . Of the three, the first two symmetries, and, therefore, conserved quantities, are also present in a lossless spiral fiber. Another symmetry common to all three structures is the mirror symmetry along the waveguide axis ($z \rightarrow -z$, C_s). Another interesting symmetry is the mirror symmetry with respect to the r - z plane ($\phi \rightarrow -\phi$, the v in $C_{\infty v}$), which allows us to classify the zero angular momentum modes according to their polarization.

In the Bragg fibers, modes with angular momentum zero can be classified as either having electric field in the plane of propagation, TM ($E_\phi = 0$), or perpendicular to the plane, TE ($E_r = E_z = 0$). Non-zero angular momentum modes ($m \neq 0$) are called hybrid and classified according to whether they are mostly TE (HE) or TM (EH). In the case of metallic waveguide, all the modes are either TE ($E_z = 0$) or TM ($H_z = 0$); there are no hybrid modes. The double degeneracy of modes with $m > 0$ and mode orthogonality suggests that the transverse polarization space is spanned by a linear combination of the two modes. In this way we get the linearly polarized TE_{11} mode, in metallic waveguide, or HE_{11} mode, in the Bragg fiber. These modes are of interest as they are the lowest energy modes and can couple efficiently to a linearly polarized Gaussian laser beam.

In the spiral fiber, rotational symmetry no longer exists. The “angular momentum”, m , will no longer be conserved and the degeneracy will be broken. Since we only have non-degenerate modes, we can no longer use linear combination to achieve the linearly polarized modes. As the mirror symmetry in ϕ disappears, so does the purely polarized mode, and we are left with only the hybrid modes EH/HE. For convenience we will call the lowest-loss azimuthally polarized mode in the spiral fiber the “ TE_{01} ” mode and the two lowest energy modes “ HE_{11} ”. A very interesting effect of the break of symmetry is a result of the break of the rotation symmetry around r , i.e. the fiber is no longer the same on both sides- when viewed from the $+z$ side a left handed spiral can be seen while a right handed spiral will be seen from the $-z$ direction. In the spiral fiber this symmetry is replaced with a planar chiral symmetry: the structure is invariant under the reflection $z \rightarrow -z$. In effect, this means that the fiber becomes directional, i.e., coupling from the $+z$ direction or from the $-z$ direction will have different results. This is due to the fact that the fiber modes in the spiral fiber from the $+z$ direction are the mirror image of the modes in the $-z$ direction; whereas, in the metallic waveguide or Bragg fiber, they are the same. It is important to note that all structures have the $z \rightarrow -z$ symmetry, but the added $\phi \rightarrow -\phi$ symmetry in the later structures means the modes on the $+z$ and $-z$ side are not only a mirror reflection of each other but are identical.

Table 1. Summary of the symmetry properties of the three structures and the ensuing modal properties

	Spiral fiber	Bragg fiber	Metallic waveguide
Symmetries	T_∞, C_s	$T_\infty, C_{\infty v}, I$	$T_\infty, C_{\infty v}, I$
Eigenstates	EH/HE	TE/TM ($m = 0$) HE/EH ($m > 0$)	TE/TM
Polarizations	Elliptical	Linear	Linear
Degeneracy	1	1 ($m = 0$) 2 ($m > 0$)	1 ($m = 0$) 2 ($m > 0$)
Directional Asymmetry	Yes	No	No

Though the structure of the spiral fiber is similar to that of the Bragg fiber, analytical analysis of the spiral fiber is much more complicated. The cylindrical symmetries that facilitated the Bragg fiber problem no longer exist in the spiral fibers. Using perturbation methods is problematic as they can only be used when the shift in boundary is much smaller than a wavelength [20], while in the spiral fiber case, the difference in structure between the Bragg fiber and the spiral fiber near the “seam”, the line along the fiber where the spiral begins, is about half a wavelength. On the other hand, the non-analytical form of the spiral (discontinuity between $\phi = 0$ and $\phi = 2\pi$) prohibits the use of methods such as transformation to curvilinear coordinates [21]. Instead we have used a commercial finite element simulation (COMSOL) to model the 2D cross section of the fiber. The materials in the simulation have complex index-of-refraction of: $2.27 \cdot 10^{-6}i$ (chalcogenide glass) and $1.57 \cdot 10^{-3}i$ (polymer). The losses of the modes obtained by the simulation are dependent on the fiber structure but are only ten times larger than the losses of a comparable Bragg fiber.

Two modes of the spiral fiber, the “HE₁₁” and the “TE₀₁” as obtained from the simulation, are shown in Fig. 2. As we have discussed before, the HE₁₁ modes of the metallic waveguide and the Bragg fiber are doubly degenerate and linearly polarized. In the spiral fiber the degeneracy is broken and the modes become elliptically polarized. We can also see that the modes of the fiber on the forward side are a mirror reflection of the modes on the backward side as expected due to the fiber symmetry. It is interesting to notice that the modes on one side are both elliptically polarized and right-handed, while those on the other side are both left-handed.

Another interesting mode is the TE₀₁ mode, the azimuthally polarized lowest-loss mode. In the metallic waveguide and Bragg fiber, this mode takes the familiar doughnut shape. In the spiral fiber the mode is still azimuthally polarized and the lowest-loss mode, but it no longer has the symmetrical doughnut shape. Instead, the mode is now asymmetric with higher intensity along one axis of the mode and lower intensity on the perpendicular axis. This asymmetry can be seen in asymmetrical fibers other than the spiral fiber, such as a Bragg fiber with an elliptical core. What makes the spiral fiber unique is the angle of the asymmetry axis with respect to the asymmetry of the structure. Whereas in the elliptical fiber, for example, the TE₀₁ axes are aligned with the core ellipse axes, in the spiral fiber the “TE₀₁” axes form a 45° angle with the “seam”. As with the “HE₁₁”, when the fiber is rotated (from +z to -z), the resulting mode is a mirror image of the original mode.

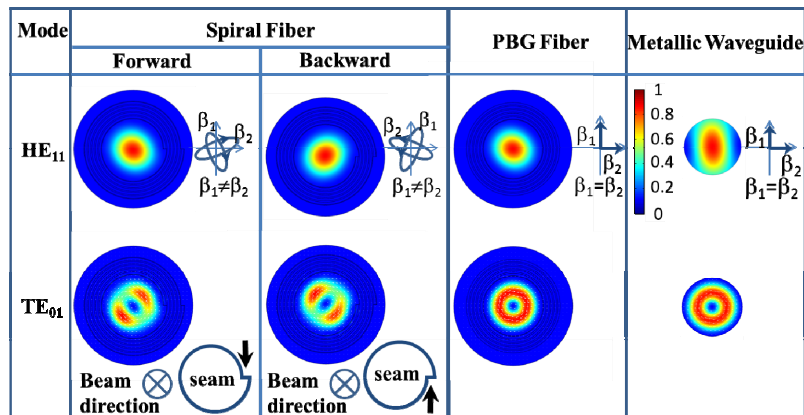


Fig. 2. Full comparison of the TE₀₁ and HE₁₁ modes between the spiral fiber, Bragg fiber and the metallic waveguide. The top pictures show the simulation results for the intensity profiles of the HE₁₁ modes with the polarization shown schematically on the axes to the right of the picture. β_i is the wavevector of the *i*th mode. The bottom pictures are the simulation results for the TE₀₁ modes. “Seam” position for the spiral fiber is indicated on the bottom as well as beam propagation direction.

We verified the simulation results by measuring the “TE₀₁” mode in our fibers. A spiral fiber was fabricated using the thermal drawing technique [22, 23]. The spiral structure is achieved by rolling a low-index of refraction material (polymer) covered by a high-index of refraction material (chalcogenide glass) on a rod and then extracting the rod. Scanning electron microscopy (SEM) pictures of the cross-section that highlight the spiral structure and the “seam” can be seen in Fig. 3. We have used fibers made from two sets of materials (poly(ether imide)/As₂S₃ or polycarbonate/As₂S₇₅) whose band gaps were centered in different wavelengths (1500nm-1600nm) and whose core sizes vary (from diameter of 50μm to 70μm, or, in wavelength units: 30λ-45λ). To measure the mode we have coupled a collimated tunable light source (Ti:Sapph laser with OPO- Coherent Mira 900 and Mira-OPO) to the fiber using a lens. We have imaged the output onto a camera (Sensors unlimited SU320) using an objective. A linear polarizer was used in all experiments to verify the output was indeed azimuthally polarized. The “TE₀₁” was generated using a method described in details in Shemuly D. *et al* [24]. In all measurements an asymmetric “TE₀₁” was seen where the axis of the asymmetry was at an angle of around 45° to the “seam”, in accordance with the simulation results. We have also measured the “TE₀₁” from both sides of the same fiber samples. In these measurements the “TE₀₁” axis was reflected with respect to the fiber rotation axis, as expected, since the “TE₀₁” from one side of the fiber should be a mirror image of the “TE₀₁” from the other side. An example of a measurement of the “TE₀₁” is presented in Fig. 4 along with the corresponding simulation result.

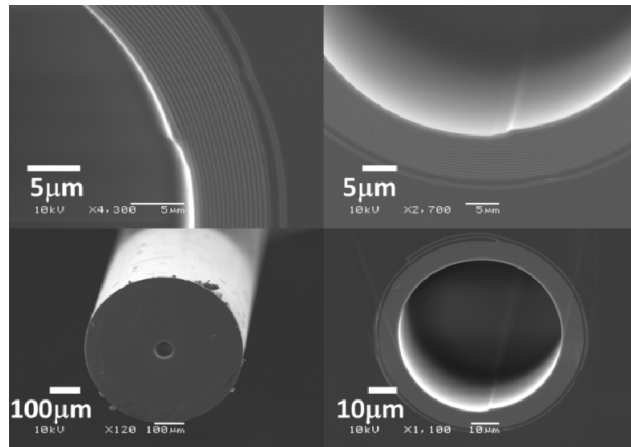


Fig. 3. SEM of a spiral fiber cross section [24]. The light gray are glass layers made of chalcogenide glass (As₂S₃) the dark gray are polymer layers and cladding made of Poly(ether imide) (PEI). The pictures on the right highlight the spiral nature of the structure and show the “seam”- the line along the core surface where the spiral begins.

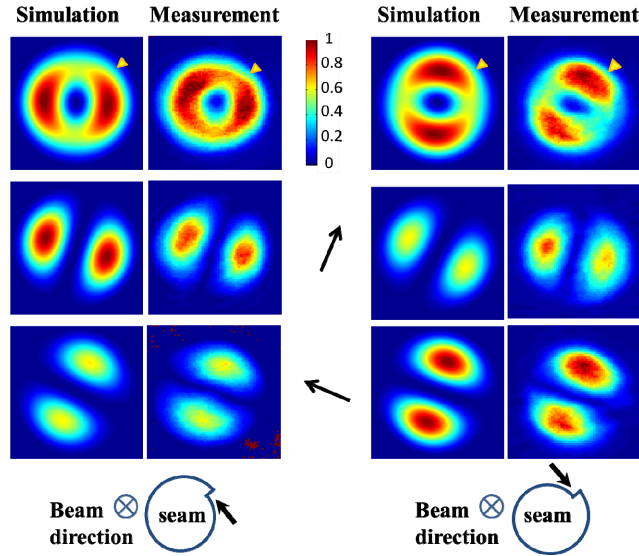


Fig. 4. Simulation and measurements [24] results of the “TE₀₁” from both sides of the fiber. The top pictures are the output without a polarizer, the two lines pictures are with linear polarizer (polarizer orientation is marked with a black arrow in the middle). The yellow triangle marks the position of the “seam”.

An interesting effect of the break of degeneracy of the “HE₁₁” modes is the appearance of polarization rotation. A linearly polarized Gaussian beam will most efficiently couple to a linear combination of the two “HE₁₁” modes. In a metallic waveguide or Bragg fiber, these modes are degenerate, and the output will maintain the input polarization plane. In the spiral fiber the modes are non-degenerate; they travel at different speeds and have different losses. This will result in a rotation of the polarization of light in a similar manner to the effect of propagation in chiral media. Since the “HE₁₁” modes from one side of the fiber are a mirror image of the modes from the other side, the direction of the polarization rotation is dependent on the direction of coupling. The polarization of the light is not only rotated but is no longer linear (as both modes are elliptically polarized).

The magnitude of the rotation and the divergence from linear polarization are dependent on several parameters: the “HE₁₁” modes' losses and propagation constants, the angle of input polarization with respect to the “seam” of the fiber, and the fiber length. At the fiber input a linearly polarized Gaussian beam will couple to the two “HE₁₁” modes: $E_{in} = A_1 E_{HE_{11}^{(1)}} + A_2 E_{HE_{11}^{(2)}} = A_1 f_1(r, \theta) e^{i\omega t} + A_2 f_2(r, \theta) e^{i\omega t}$, where E_{in} is the input beam field, $E_{HE_{11}^{(i)}}$ ($i = 1, 2$) are the “HE₁₁” modes' fields, A_i are the linear sum coefficients, f_i ($i = 1, 2$) describes the vector fields' dependence on r and θ , and ω is the frequency (assuming we are working at a single frequency). After propagating through the fiber, each mode will accumulate different attenuations: $E_{out} = A_1 f_1(r, \theta) e^{i\omega t} e^{-ik_1 z} + A_2 f_2(r, \theta) e^{i\omega t} e^{-ik_2 z}$, where k_i ($i = 1, 2$) is the complex wave vector component in z , which can be described as $k_i = \beta_i - i\delta_i$, where β , the real part, is the propagation constant, and δ , the imaginary part, is the mode's loss. The capability of the fiber to rotate and change the polarization of light could enable in-fiber polarization rotation and manipulation without the need to couple light in and out from a fiber to bulk optical components.

Sub-wavelength chiral structures have shown fascinating optical effects, including negative refraction and optical activity. However, typically, their structure's thicknesses have been limited to a few wavelengths [10, 11, 25, 26]. This limitation only allows for a very short length over which interaction between the electromagnetic wave and the chiral

structure's eigenstates can occur. Waveguides, on the other hand, allow for extended interaction length; however, for the most part they do not exhibit chiral symmetry. Here we demonstrated a spiral fiber structure that has unique chiral properties due to its lack of symmetry and the small modal losses. Using symmetry considerations and finite element simulation we have studied the modal properties of this new structure. We have shown experimentally the effect of the chiral symmetry on the “TE₀₁” mode and highlighted the interesting *in-principal* asymmetric polarization rotation in the structure.

Acknowledgments

The authors would like to thank Professor Joannopoulos for his help and encouragement. This work was supported in part by the MRSEC Program of the US NSF under award number DMR-0819762 and also in part by the US Army Research Office through the ISN at MIT under contract no. W911NF-07-D-0004.